IMS INFRASOUND MONITORING TEST SITE AT TRAFELBERG, AUSTRIA: PRELIMINARY RESULTS FROM IN-SITU RESPONSE MEASUREMENTS OF INFRASOUND ELEMENTS

Thomas Gabrielson[1], Georgios Haralabus[2], and Stefi Stefanova[2]

Penn State University[1] and the Comprehensive Nuclear-Test-Ban Treaty Organization[2]

ABSTRACT

The International Monitoring System (IMS) of the Comprehensive Nuclear Test-Ban Treaty Organization (CTBTO) has a unique infrasound test site (I99AT) with four wind-noise-reduction pipe-array systems in close enough proximity to allow simultaneous measurements under similar environmental conditions. It was designed as a facility to study the effectiveness of various wind-noise-reduction systems so it is clear of trees, vegetation, or other wind breaks. The persistent winds presented a challenge for response measurement by reference-microphone comparison; however, there were several suitable periods during the eight days of continuous recording from 19 May to 27 May 2010.

Reasonable estimates for the magnitude and phase response of all four infrasound elements at I99 were made from 0.008 Hz to several Hz. For all four elements, from 0.01 to 0.1 Hz, the measured magnitude and phase correspond closely to the manufacturer's specifications for the MB2005. Above 1 Hz, the effects of the pipe system produce a significant change in the phase response compared to the MB2005. Below 0.01 Hz, the phase also changes somewhat faster than expected. A preliminary investigation of the effects of non-acoustic turbulence and the associated scale sizes was performed and an apparent drop in the magnitude response of the larger elements below 0.08 Hz was tentatively associated with area-averaging of non-acoustic pressure fluctuations. Finally, in windy conditions, the large hexagonal element showed higher spectral levels from 0.2 to 3 Hz than the small element.

OBJECTIVES

This progress report covers eight days of reference-microphone measurements at the I99AT infrasound test bed in Trafelberg, Austria. The I99 infrasound test bed comprises four complete pipe-array elements. Two of the elements are rosettes – 18 and 36 meters overall dimension – and are placed so that their geometric centers are coincident. The other two elements are close-packed hexagonal configurations – 18 and 36 meters overall – also with coincident geometric centers. They are located in an area surrounded by trees and hills; however, there are no trees or other vegetation in the immediate area of the elements.

Since the hexagonal and rosette systems are only 44 meters apart, reference microphones could be deployed at all four systems for simultaneous evaluation. Four reference microphones were used with three microphones in a triangular configuration at the hexagonal-pair center and the fourth microphone at the rosette-pair center. Halfway through the deployment, the positions of the three microphones and the single microphone were reversed. The overall configuration is shown in Figure 1 below. This configuration of I99 elements and reference microphones meant that a number of different spatial scales could be investigated under nearly the same conditions.

For part of the deployment period, two portable systems provided by the PTS were placed near the center of the rosette pair. One of these systems was run with its port open, the other with its port connected by a length of hose to a quad-plate reference port. The I99 systems and the portable systems all use the MB2005. The reference microphones are all GRAS 40AZ cartridges with 26CG preamplifiers and a custom power supply and gain stage.

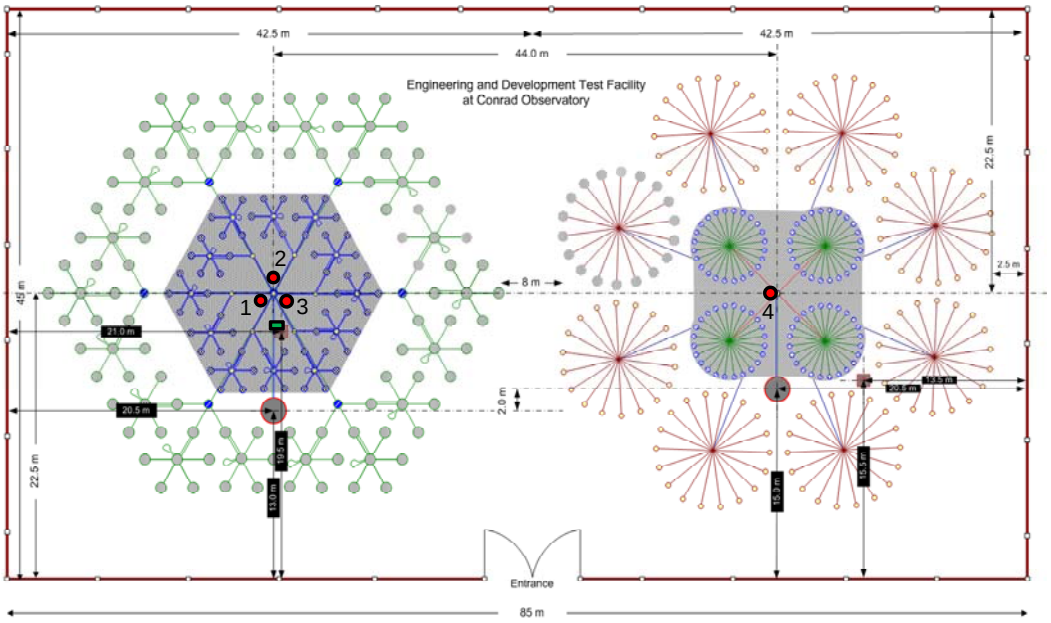

Figure 1. Schematic diagram of the elements at I99AT and the reference microphones. The two hexagonal close-packed arrays are on the left; the two rosette systems are on the right. For dimensional reference, the two sets of elements are 44 meters from center to center. The Reference Microphones 1-3 (red) were placed on a 1.5-meter radius circle coincident with the geometric center of the element. Reference Microphone 4 was placed close to the center of the rosette systems. The green rectangle represents the data-acquisition hardware. For the second half of the deployment, the three microphones were moved to the rosette and the single reference to the hexagonal element. During the second half of the measurement period, two portable microbarometer systems were deployed near the center of the rosette pair. Results from those systems will be included in a later report. (Site diagram from P. Grenard.)

The reference microphones were installed on 19 May 2010 (Day 139) with recording started at 10:11 UTC. Data were recorded continuously until 27 May 2010 (Day 147) at 08:43 UTC for a total of about 190 hours. The first half of the deployment period was characterized by moderate to high gusty winds and periods of heavy rain; during the second half, the winds dropped somewhat but the periods of rain continued. Consequently, the reference-microphone data are often dominated by wind noise. There were, however, several periods of sufficiently calm winds that a response reconstruction could be performed.

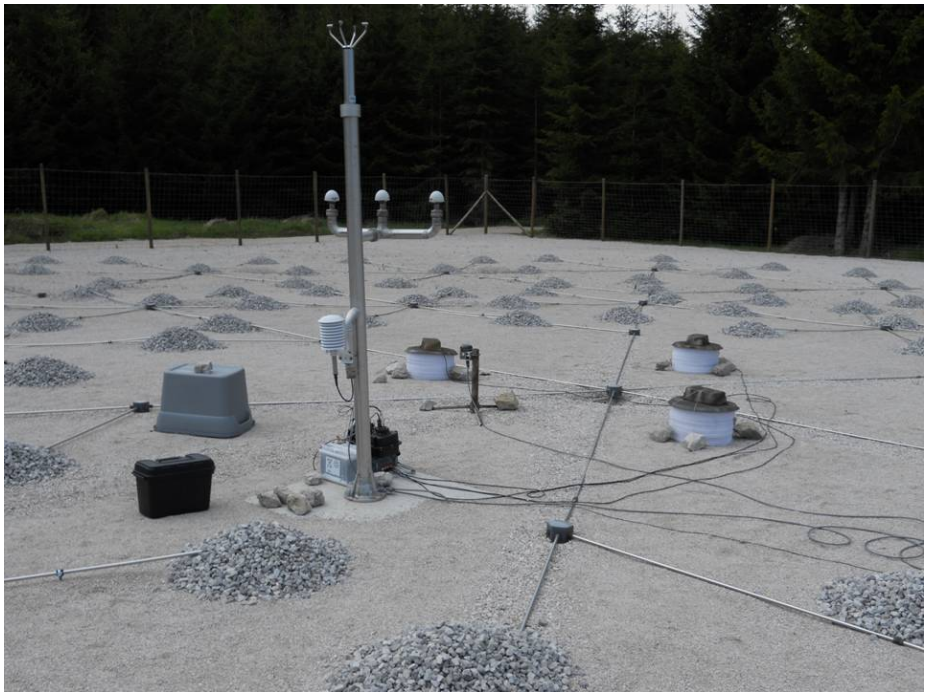

Figure 2. Deployment of the three reference microphones on a 1.5-meter radius circle centered on the hexagonal element pair. The three microphones in their wind screens are to the right of the meteorological instrumentation tower and the data acquisition unit is at the base of that tower.

Figure 3. View from near the center of the hexagonal elements toward the rosette elements. The pad on which the four I99 elements are installed is clear of all vegetation. The forested area starts somewhat outside the fenced pad.

Basic Frequency Response Estimation

Periods with low winds were rare; however, there were quiet periods on both 25 May and 27 May in the early morning hours. The period used here was about 50 minutes long starting at 01:42 UTC on Day 145 (25 May). At this time, Microphones 1-3 were located at the center of the hexagonal element pair and Microphone 4 was located at the center of the rosette pair.

The I99 elements have the following general characteristics:

Type	Channel Designation	Overall Size	Number of Inlets
small rosette	V1-BFH	18 m	96
large rosette	V1-BFL	36 m	144
small hexagon	V2-BFH	18 m	72
large hexagon	V2-BFL	36 m	108

For response estimation, the averaged cross-spectral density between the relevant I99 element and the co-located microphone (or microphone combination) was calculated using 10-minute records overlapped by 50%. The averaged auto-spectra for the I99 element and for the reference channel were also calculated. From these spectral densities, the coherence was calculated and the response of the I99 element was calculated. The response calculation also depends on the laboratory calibration of the reference microphone system. Details of the response estimation procedure are available elsewhere.

When three microphones are used, their outputs are summed (in the time domain), which forms a virtual microphone with a phase center at the geometric center of the I99 element. When a single microphone is used, that microphone is placed as close as practical to the geometric center of the element. The issue of physical offset from the geometric center of the I99 element is only significant near the upper end of the frequency range; even there, the error from a one- to two-meter offset is small. The virtual microphone formed by the sum of three microphones does have a small degree of noise rejection compared to a single microphone.

The next eight figures show the magnitude and phase estimates for each of the four I99 elements. Those plots are coded by coherence value. The blue curve is the response estimate made regardless of the value of coherence. The red circles correspond to coherence greater than 0.9 and the black circles to coherence between 0.75 and 0.9. This coding gives some indication of the reliability of the results. The blue curve should be ignored; the red circles should be reliable estimates. The solid green curve is the expected response[1] of the MB2005 and digitizer anti-aliasing filter. Differences between the green curve and the red/black circles indicate either response deviations in the microbarometer system or effects of the wind-noise-reduction piping network. The effects of the piping network are expected to be most significant toward the higher frequencies.

[1] MB2005 response from the Martec CEA MB2005 User Manual, 14643-B January 2006, section 5.5.1.

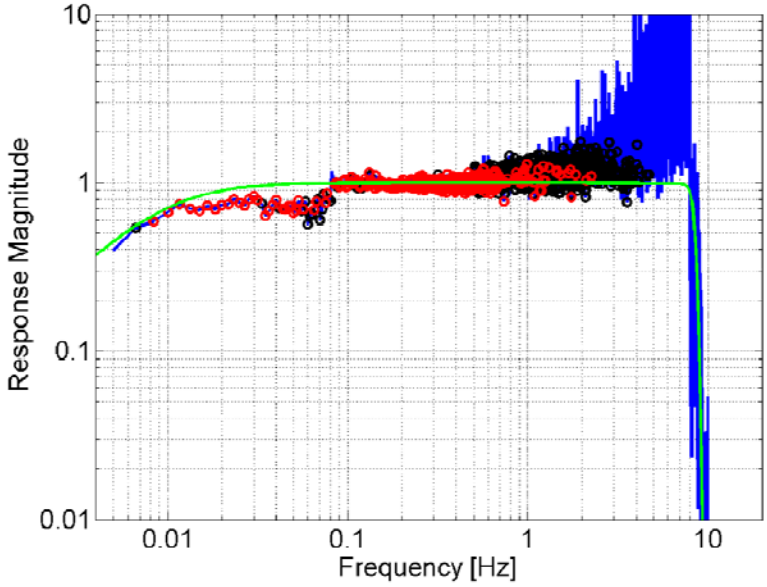

Figure 4. Magnitude response calculation for the large hexagonal element (V2-BFL). The calculation represents a 50-minute period starting at Day 145 01:42 UTC. The reference channel is the sum of Microphones 1, 2, and 3. The apparent offset in magnitude response that appears from 0.01 to 0.08 Hz is discussed in the text below.

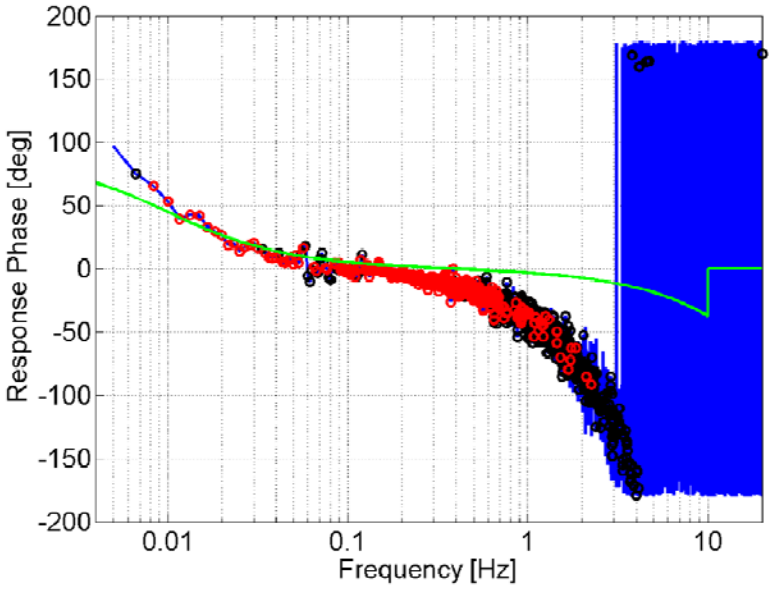

Figure 5. Phase response for the large hexagonal element (V2-BFL) corresponding to the magnitude plot above. The effects of the pipe network show up most clearly in the phase response as a departure from the MB2005 phase above 0.1 Hz. Notice that there is no offset in the phase in the 0.01 to 0.08 Hz region but there is an increase in the scatter near 0.08 Hz.

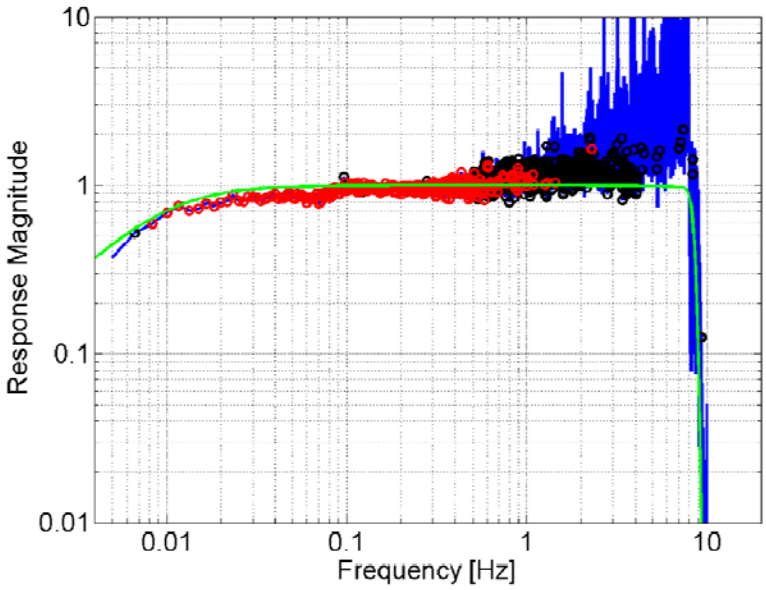

Figure 6. Magnitude response calculation for the small hexagonal element (V2-BFH). The calculation represents a 50-minute period starting at Day 145 01:42 UTC. The reference channel is the sum of Microphones 1, 2, and 3. Notice that the apparent offset in magnitude response below 0.08 Hz is considerably smaller than for the large element (V2-BFL).

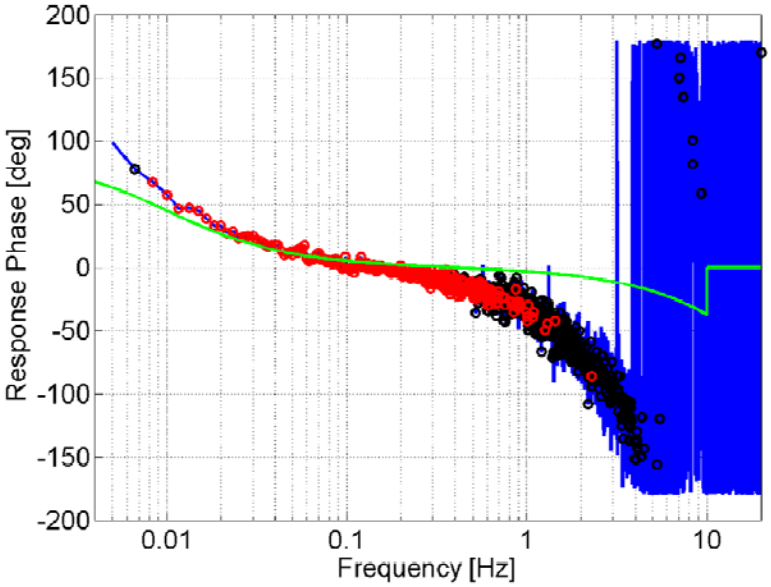

Figure 7. Phase response for the small hexagonal element (V2-BFH) corresponding to the magnitude plot above. The effects of the pipe network show up most clearly in the phase response as a departure from the MB2005 phase above 0.1 Hz.

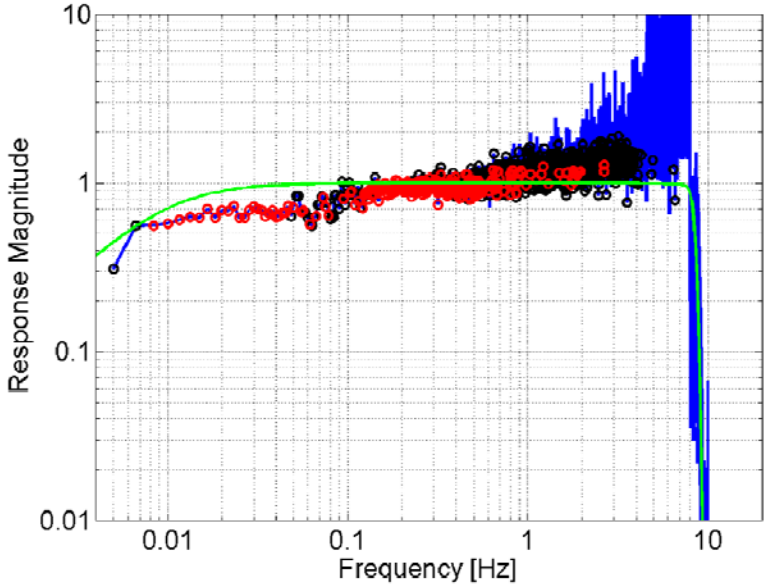

Figure 8. Magnitude response calculation for the large rosette element (V1-BFL). The calculation represents a 50-minute period starting at Day 145 01:42 UTC. The reference channel is Microphone 4. An apparent offset in magnitude response, similar to that for the large hexagonal element, appears in the 0.008 to 0.08 Hz range.

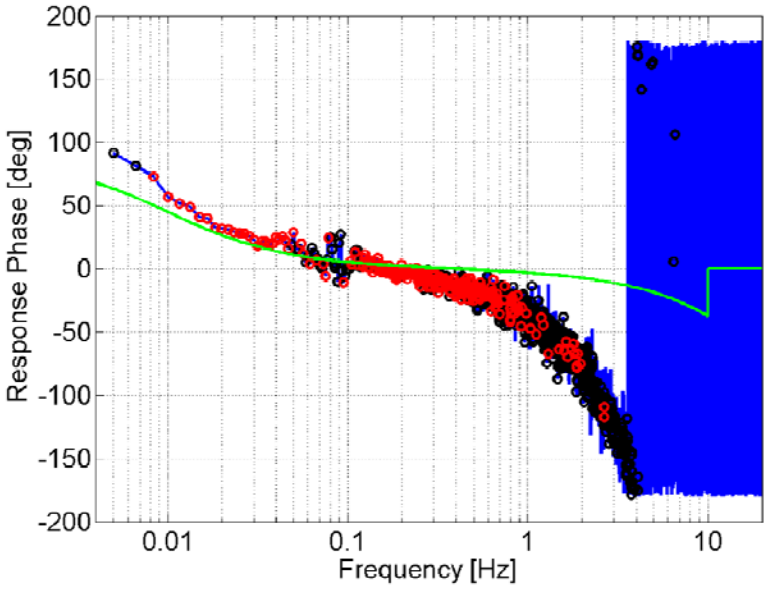

Figure 9. Phase response for the large rosette element (V1-BFL) corresponding to the magnitude plot above. Notice the increase in scatter near 0.08 Hz but the lack of an offset. The effects of the pipe network show up most clearly in the phase response as a departure from the MB2005 phase above 0.1 Hz.

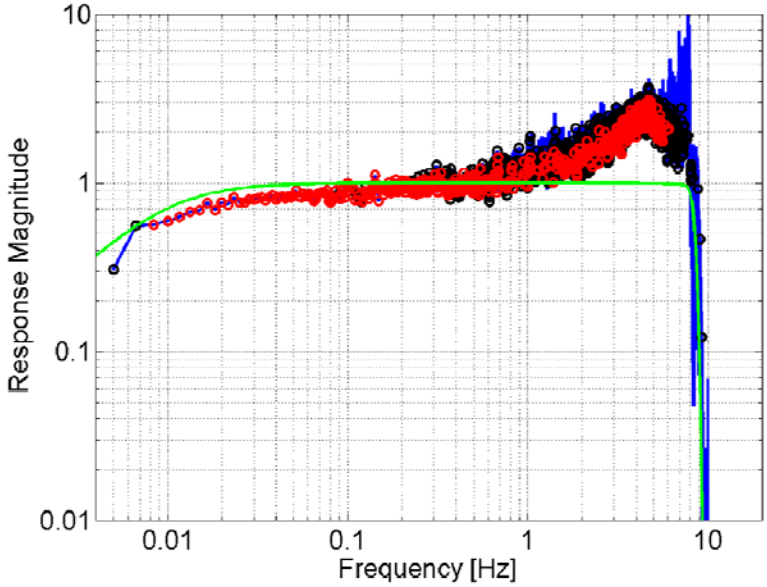

Figure 10. Magnitude response calculation for the small rosette element (V1-BFH). The calculation represents a 50-minute period starting at Day 145 01:42 UTC. The reference channel is Microphone 4. For this element, the magnitude response shows an increase at the high-frequency end that is characteristic of a resonance in the system.

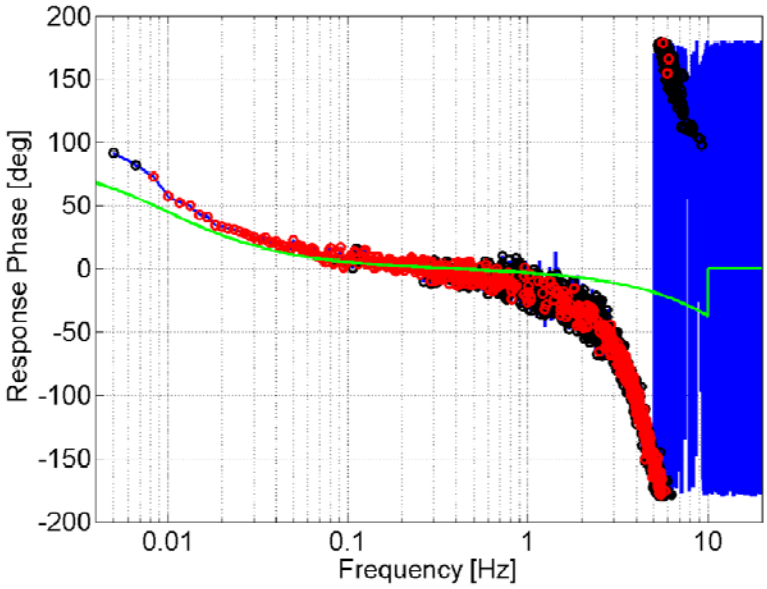

Figure 11. Phase response for the small rosette element (V1-BFH) corresponding to the magnitude plot above. The phase at higher frequencies is consistent with a resonance. Compared to the other phase plots, the phase departs more slowly above 0.1 Hz initially; however, the rate of change of phase at the highest valid frequencies is greater than for the other elements.

Influence of Non-Acoustic Pressure Fluctuations

Perhaps the most striking feature of the response estimates is the apparent jump in magnitude near 0.08 Hz for both of the 36-meter elements (with some suggestion of a smaller magnitude shift in the two 18-meter elements). In attempting to understand this behavior, it is important to identify the pressure field being sensed at different frequencies. The plot below is a typical coherence plot; the coherence is computed between the reference channel and the I99 element channel.

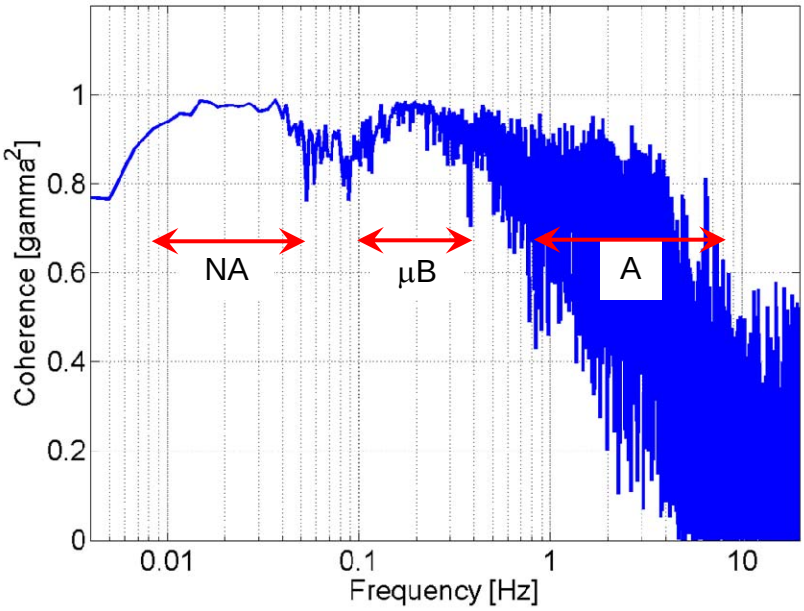

Figure 12. Coherence between the co-located reference microphone (Microphone 4) and the large rosette (V1-BFL). If the wind is low enough, the region between 0.1 and 0.4 Hz is often dominated by microbaroms (μB). Frequently, the region above the microbarom range is dominated by anthropogenic (A) sources of sound. At the I99 site, excitation above 1 Hz was generally weak. Although less well established, the region below 0.1 Hz may be dominated by non-acoustic (NA) pressure fluctuations advected past the sensor by wind.

The microbarometers and the reference microphones respond to pressure fluctuations regardless of their cause. Ideally, we would like to excite the systems with acoustic waves over the entire range of frequencies; however, this is not always possible. Certainly, when the wind is strong, the entire spectrum may be registering the passage of non-acoustic turbulence-related fluctuations. In this case, we would expect low coherence as long as the scale size of the turbulence is smaller than the wind-noise-reduction system.

Observations at a number of infrasound sites (including I99) suggest that there are several distinct regions of source mechanism across the spectrum. When winds are weak (or the system is well shielded by trees and undergrowth), the ambient background from about 0.1 Hz and above seems to be dominated by acoustic pressure fluctuations – microbaroms from 0.1 to 0.4 Hz, then various sources (typically anthropogenic) of acoustic waves above that.

Under exceptionally calm conditions, the region below 0.1 Hz may be the result of acoustic disturbances but it seems likely that in many cases, the ambient background below 0.1 Hz is the result of local non-acoustic pressure fluctuations. These non-acoustic fluctuations travel with the local wind rather than at the speed of sound.

Consequently, their effective "wavelength[2]" at a given frequency can be quite short and the area averaging of pipe-array networks can influence the apparent received level.

With respect to non-acoustic pressure fluctuations, then, the relationship of the scale size of these fluctuations to the dimensions of the sensor is critical. With a steady average wind, a pressure disturbance with large physical dimension would appear at a lower frequency than a disturbance with small physical dimension. We would expect the following:

(a) Below some frequency, the pressure disturbance "wavelength" would be larger than the pipe network and both the pipe system and the smaller reference microphone would respond in like manner with high coherence.

(b) Above that frequency, the spatial scale of the pressure fluctuation becomes smaller than the wind-noise-reduction pipe network but still larger than the reference microphone wind screen. Here, the pipe network samples both positive and negative phases of the pressure fluctuation and the apparent level at the microbarometer is reduced over that sensed by the reference microphone. The magnitude of the response of the element would appear to drop.

(c) At higher frequencies, the spatial scale of the pressure fluctuations would drop below the effective spacing of the inlets of the wind-noise-reduction network. The noise "gain" of the pipe network would reach its limiting value.

(d) Eventually, the spatial scale would drop below the size of the reference microphone wind screen and the reference microphone wind screen would start to average out (and, therefore, reduce) the fluctuations.

If wind noise dominates over the entire spectrum, then we would see low coherence over most of the spectrum; however, the coherence would still be high at frequencies sufficiently low that the pressure-fluctuation spatial scale was larger than the wind-noise-reduction pipe network. For example, Figure 13 below shows the coherence between the reference-microphone channel and one of the I99 elements during a period of moderate wind. Below 0.1 Hz, the coherence is high. If this region is dominated by non-acoustic pressure fluctuations, then the coherence should drop significantly if the reference microphone is displaced from the center of the I99 element. This drop in coherence is shown in Figure 14 for which Microphone 2, located 44 meters from the V1-BFH element center, is used as reference. The spatial scale[3] of non-acoustic disturbances below 0.1 Hz is smaller than the offset of the reference so the coherence drops. For an acoustic field below 0.1 Hz, the coherence would remain high even with the 44-meter offset in reference microphone.

[2] It is more conventional to describe the spatial scales in terms of wave number; however, wavelength is more intuitive in the context of area averaging. The wavelength is 2π divided by the wave number whether the disturbance is acoustic or not.

[3] To be precise: the coherence length.

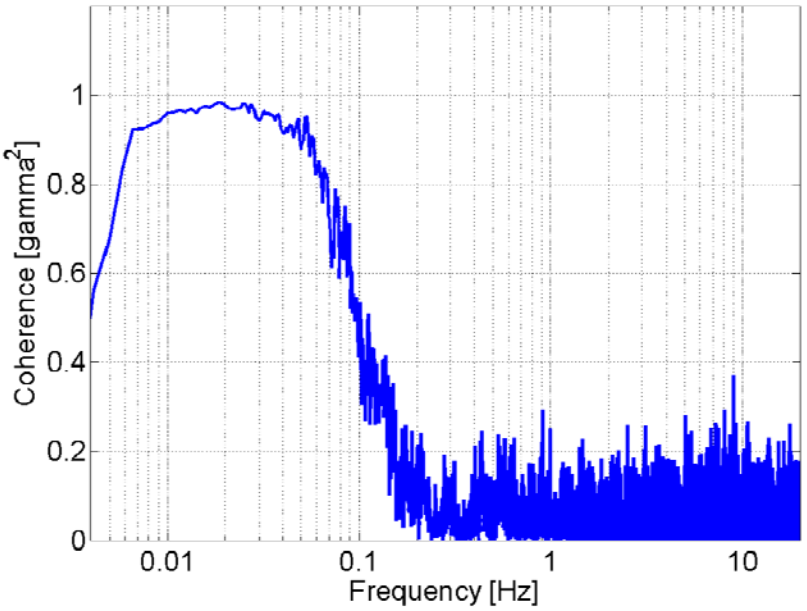

Figure 13. Coherence between the co-located reference microphone (Microphone 4) and the small rosette (V1-BFH) during a period of moderate wind. The coherence is still high below 0.07 Hz but is very low above 0.1 Hz.

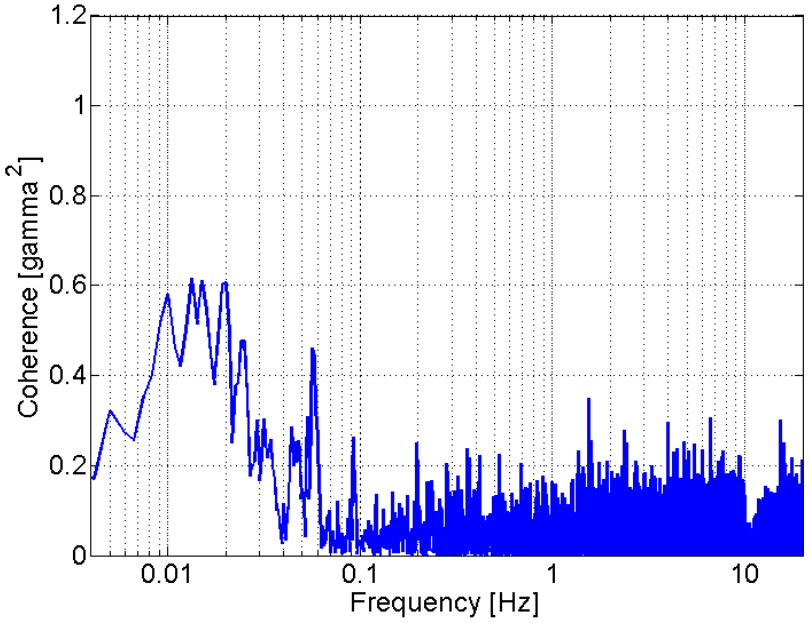

Figure 14. Coherence between a reference microphone (Microphone 2) 44 meters from the center of the small rosette and the small rosette (V1-BFH) during a period of moderate wind. The coherence is much lower below 0.1 Hz than that shown in Figure 13. If the ambient below 0.1 Hz was acoustic, the coherence would still be high.

Another approach for considering the impact of spatial scales of turbulence is an examination of the pressure spectral density. In the figure below, the pressure spectral densities of the small rosette (V1-BFH) and of the co-located reference microphone are shown.

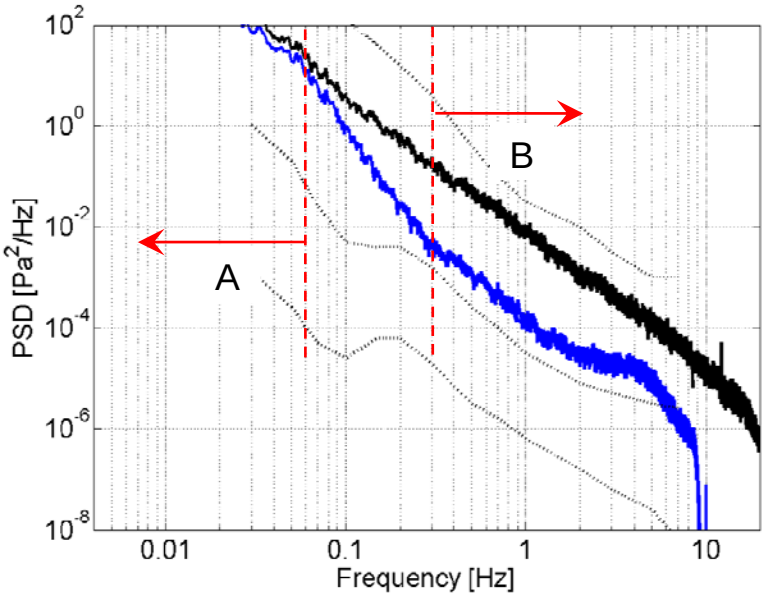

Figure 15. Pressure spectral densities for the small rosette (blue) and for the co-located reference microphone (black) for the same windy period as for Figures 13 and 14. Below 0.06 Hz (A), the spectra are nearly identical; from 0.3 to 2 Hz (B), the spectra are parallel.

Notice at the lowest frequencies that the spectral densities for the reference microphone and for the I99 element are nearly the same. In this example, below about 0.06 Hz, the scale sizes of the non-acoustic pressure fluctuations are large enough that the small rosette is too small to be effective in area averaging those fluctuations. When that happens, the single reference microphone and the extended-area rosette produce virtually the same result. Above 0.06 Hz, the turbulence scale size drops below the overall size of the rosette and the rosette spectral density starts to drop below that of the reference microphone – the result of averaging over the rosette's spatial extent. Once the scale size of the turbulence drops below the effective inlet spacing[4] of the rosette, the area averaging reaches its maximum value and the rosette spectrum parallels the microphone spectrum. For this example, this occurs at about 0.3 Hz.

If the scale-size argument is valid, then the large rosette would maintain area averaging to lower frequency (perhaps a factor of two lower – 0.03 Hz – if the averaging scales directly with overall dimension) than the small rosette. Figure 16 – comparable to Figure 15 but for the large rosette – shows that this may be the case. Figure 16 also shows the additional degree of inlet averaging (as evidenced by the larger difference in levels) above 0.3 Hz associated with the larger number of inlets in the large rosette (144 compared to 96).

[4] For a non-uniform inlet distribution, there is some question as to the appropriate value for the "effective" inlet spacing.

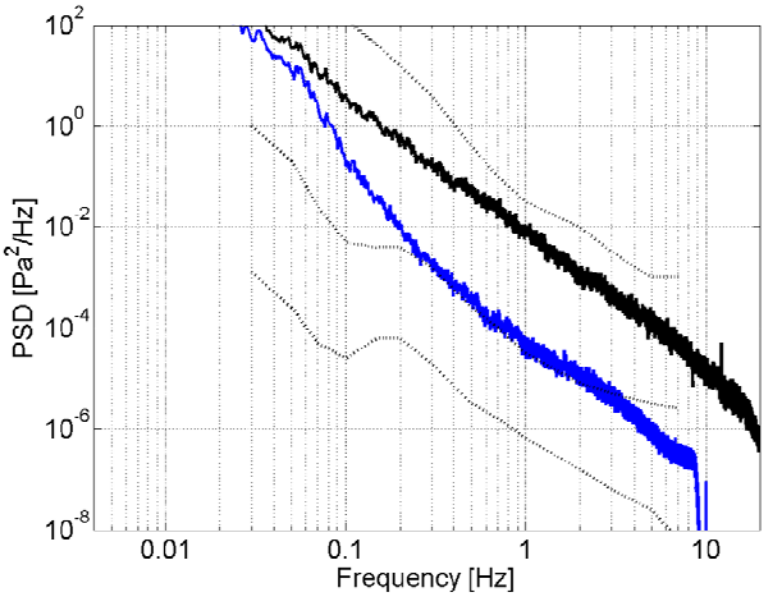

Figure 16. Pressure spectral densities for the large rosette (blue) and for the co-located reference microphone (black) for the same windy period as for Figure 15. Notice that the blue curve is lower for the large rosette than for the small rosette in the region where it parallels the single-microphone spectrum. Further, notice that the blue curve approaches the black curve at a lower frequency than for the small rosette.

If it is true (for these measurements) that the source mechanism below 0.1 Hz is non-acoustic pressure fluctuation, then the apparent frequency response of the I99 element would be affected. In that case, we would see the actual MB2005 response at the very lowest frequencies since, for those frequencies, the scale size of the fluctuations is larger than the pipe array. As the frequency increases, the scale size of the fluctuations decreases (assuming roughly constant average wind) and, at some point, the extended pipe array starts to average over positive and negative fluctuations. This would appear as a decrease in the magnitude of the response; however, the basic response of the MB2005 is still increasing toward its "mid-band" value; therefore, the net effect is a roughly flat response somewhat below the expected acoustic response.

Once the frequency has increased to the point where microbaroms start to dominate, the dominant source mechanism becomes acoustic, the wavelength is very large compared to the pipe array, and there is no longer any reduction in response from averaging over the much shorter "wavelength" non-acoustic fluctuations. In the frequency response reconstruction, this would appear as a jump in the response magnitude. That jump should be larger for the larger pipe arrays (since the onset of area averaging occurs at a lower frequency for the larger systems) and that is, in fact, what appears when comparing Figure 4 to Figure 6 or Figure 8 to Figure 10.

The actual acoustic response is correctly estimated when the source mechanism is acoustic or when the scale of the non-acoustic fluctuations is so large that the responses of the extended pipe array and the single microphone (or virtual microphone) are equivalent.

Figure 4 above illustrates this the most clearly. At the lowest frequencies, the estimated response is very close to the expected MB2005 low-end response. Above the "jump" in magnitude response at 0.08 Hz, the response is, again, close to the expected mid-band response. In the region between 0.01 and 0.08 Hz, the competing effects of area averaging by the extended pipe array and the low-frequency roll-off of the MB2005 produce a relatively flat response that is about 20% lower than the expected mid-band response.

It is important to recognize that the measured *phase* response is not affected by area averaging of non-acoustic fluctuations. The phase response does not reflect any noticeable discontinuity at the same frequency as the magnitude jump. This is one of the most compelling arguments that the magnitude jump is not a "real" jump in the

acoustic response of the system. If the actual acoustic response showed a jump in magnitude, causality would require a corresponding change in the phase response. In this case, *the magnitude jump reflects a difference in the structure of the field external to the pipe array*. However, because the phase centers of the reference microphone and of the I99 element are coincident, the phase response is estimated accurately.

In fact, from observations at a number of sites, the phase appears to be a more reliable estimator of true acoustic response than the magnitude. In addition to the bias associated with area averaging of non-acoustic fluctuations, the magnitude estimate can be biased by incoherent noise whereas incoherent noise only increases the scatter of the phase estimate without introducing a bias. Consequently, the phase can be used to guide reconstruction of the actual acoustic response.

We can gain further insight into the impact of scale size by exploiting the co-location of two pipe arrays of different size. If the pressure field below 0.1 Hz is predominantly non-acoustic pressure fluctuations with small "wavelength" (i.e., large wave number), then the larger of the two pipe systems should appear to drop somewhat in response compared to the smaller system from the lowest frequencies up toward 0.1 Hz. Figure 17 below was constructed by taking the smaller of the two pipe systems as the reference and calculating the response of the larger array relative to the smaller one. For acoustic waves, the relative response should be one at all frequencies. Notice, however, that below 0.1 Hz, we see a drop in response that is consistent with the onset of area averaging for the larger system at a lower frequency than for the smaller system.

For both the rosette-to-rosette comparison and for the hexagonal-to-hexagonal comparison, the coherence shows a dip just below 0.1 Hz that is consistent with a change in the nature of the pressure field from non-acoustic pressure fluctuations below 0.1 Hz to microbaroms above 0.1 Hz. At the lowest frequencies and above 0.1 Hz, the relative magnitude of the response is one for both pairs of pipe arrays. (Also, notice that, above 1 Hz, the relative response for the rosette systems shows the difference in high-frequency response illustrated explicitly in Figure 10.) The high coherence above 10 Hz is an artifact introduced by the up-sampling process[5] applied to the element data.

[5] The reference microphone signal is sampled at 250 samples per second and the I99 element signal is sampled at 20 samples per second. In order to characterize the element response through the anti-alias filter roll-off at 8 to 10 Hz, the data are processed at 50 samples per second. The reference signal is down-sampled and the element signal is up-sampled so that their sample rates match.

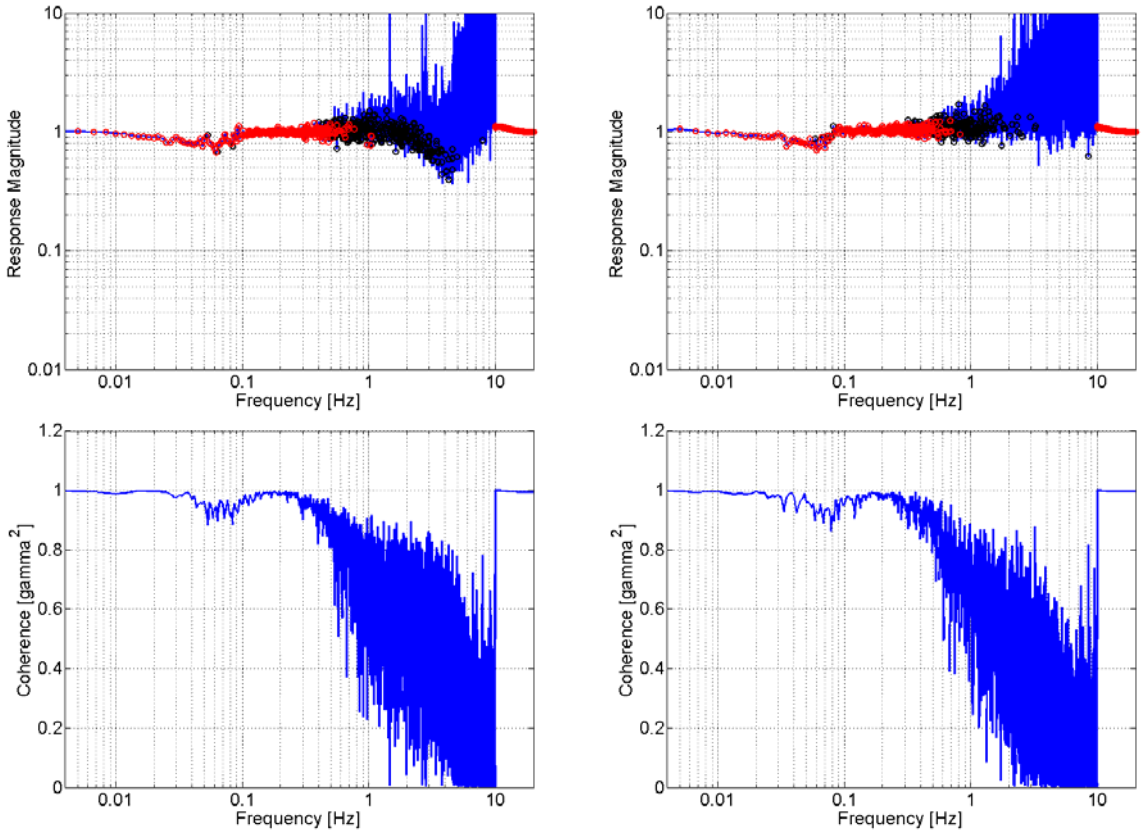

Figure 17. Magnitude response reconstructions for the larger pipe arrays using the corresponding smaller pipe array as the reference. Upper left: magnitude response of V1-BFL relative to V1-BFH; lower left: corresponding coherence; upper right: magnitude response of V2-BFL relative to V2-BFH; lower right: corresponding coherence. (The high coherence above 10 Hz is an artifact introduced by the up-sampling of the original data.)

Extended Low-Frequency Response Estimation

If these speculative conclusions regarding non-acoustic fluctuations are valid, then the very lowest frequency response can be determined even in windy conditions. To illustrate, we can take a long period (12 hours) during relatively strong winds, average using longer records (4800 seconds), and concentrate on the low-frequency response. This was done for the small hexagonal element in the figures below. Figure 18 shows the coherence; Figure 19 and Figure 20 give the magnitude and phase response. Even though this period is much "noisier" than the period selected for the response estimates in Figures 4-10, the low-frequency results compare closely with the corresponding results in Figures 6 and 7.

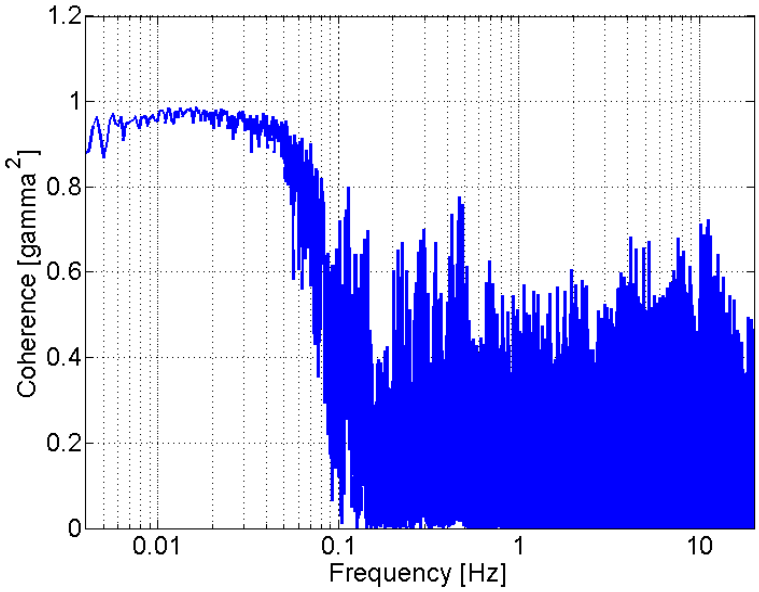

Figure 18. Coherence between the small hexagonal element and the virtual reference microphone for a 12-hour period of moderate winds. The record length is lengthened to 80 minutes in order to better resolve the lower frequencies. The coherence is greater than 0.9 from 0.006 to 0.05 Hz.

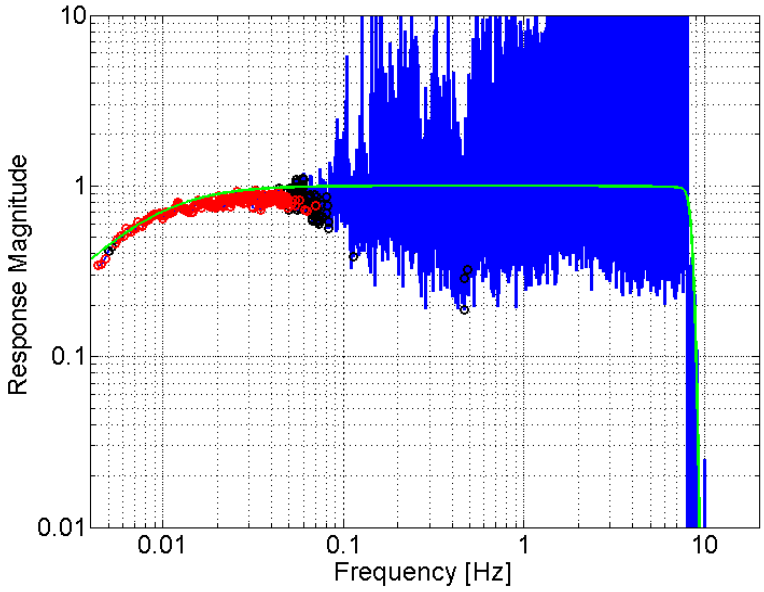

Figure 19. Magnitude response reconstruction for the small hexagonal element for low frequencies. Compare this result to the corresponding result in Figure 6.

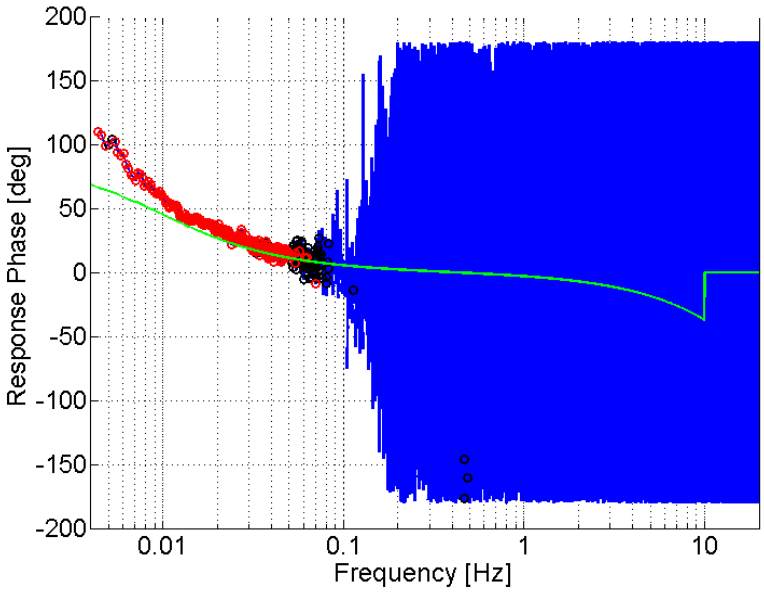

Figure 20. Phase response reconstruction for the small hexagonal element for low frequencies. The departure from the expected MB2005 response (green) at the lowest frequencies suggests the presence of another pole in the low-frequency response. Compare to Figure 7.

Element-to-Element Comparisons

An examination of the pressure spectral densities for all four I99 elements is worthwhile. One-hour averaged (100-second records) spectra were generated for every hour of the measurement period. The figure below is typical of those results. Below 0.1 Hz, the spectral density seems directly related to the overall size of the array with the two 18-meter arrays giving about the same levels and the two 36-meter arrays giving about the same levels. Above 0.1 Hz, the effects of averaging over the inlet geometry control the spectral shape.

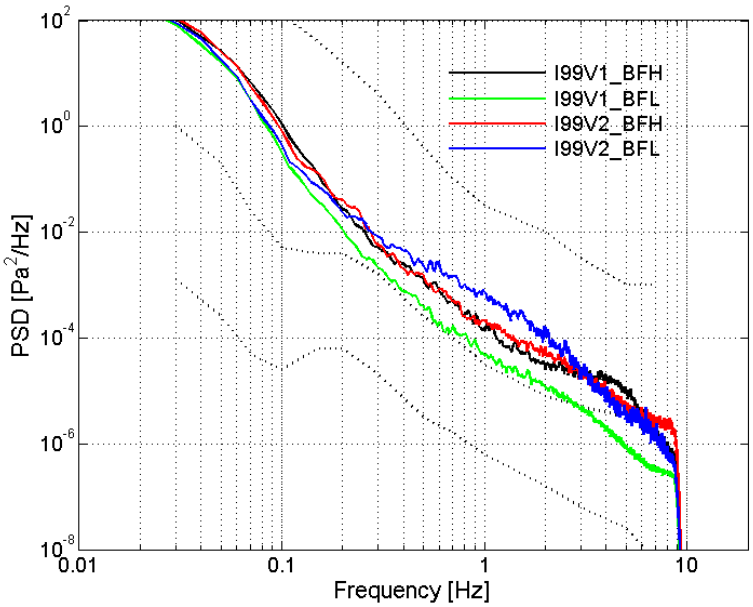

Figure 21. Pressure spectral densities from the four I99 elements. The period of 6 hours starting at 00:00 UTC on 21 May (Day 141) was a period of strong and gusty wind as evidenced by the levels shown here. The four elements are: 18-meter rosette (V1-BFH, 96 inlets), 36-meter rosette (V1-BFL, 144 inlets), 18-meter hexagonal (V2-BFH, 72 inlets), and 36-meter hexagonal (V2-BFL, 108 inlets). The dotted black lines are low-, medium-, and high-noise averages from many IMS arrays (Bowman, Baker, and Bahavar, 2005). Compare this plot to Figure A-1 in Appendix A for an example of much lower wind conditions.

A surprising result is that the highest spectral levels above 0.3 Hz belong consistently to the *larger* hexagonal array. This may suggest a problem in the large hexagonal array or it may be associated with the specific inlet geometry. We can synthesize another array by combining the large and small hexagonal array outputs (as a time-domain average weighted by the number of inlets in the two "sub-arrays"). This synthetic array has a more uniform distribution of inlets than the large hexagonal array – the large array has a void in the center (see Figure 1).

As Figure 22 shows, the synthetic array (with 180 inlets) produces a spectral density generally as low as or lower than either the small or large hexagonal array. This suggests that there is no fault in the large hexagon but, rather, that the spectral levels depend in a more complicated manner on the geometry of the inlet distribution than a simplistic N-inlet average suggests.

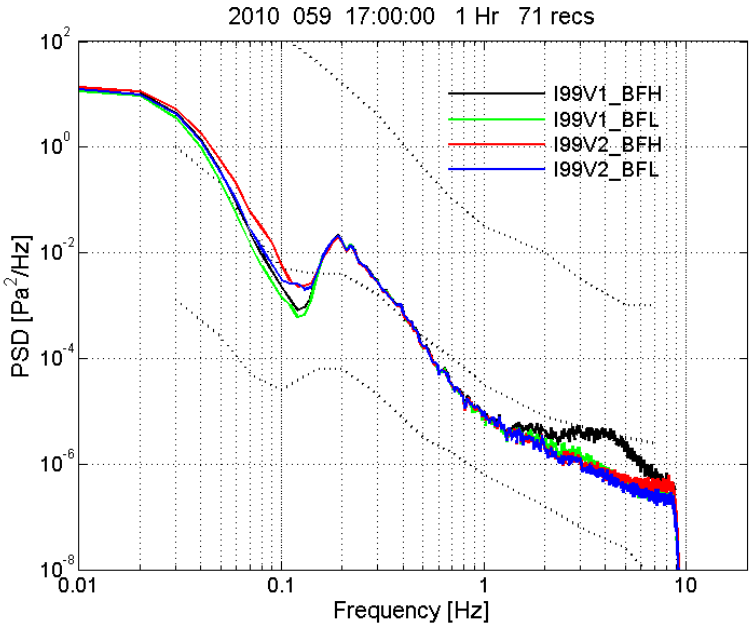

Figure 22. Pressure spectral densities for the four elements at I99 for a period of relatively low wind from 01 March 2010. Compare this to Figure 21 in the text. Notice that the small rosette (V1-BFH) appears to have a higher response above 1 Hz than the other elements. Notice also how closely matched the elements are from 0.13 to 1.2 Hz and the divergence below 0.13 Hz. This further supports the hypothesis that the region below 0.1 Hz is non-acoustic even for low-wind conditions.

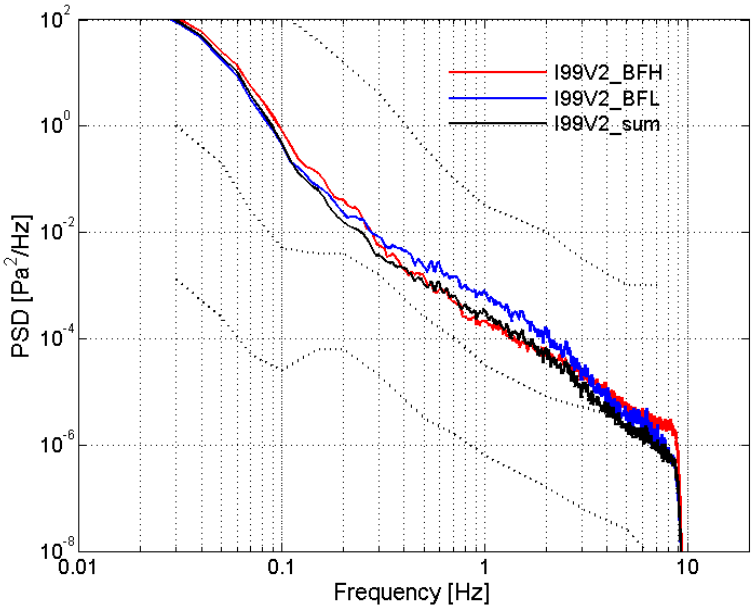

Figure 23. Pressure spectral densities from the two hexagonal I99 elements and a synthetic array formed by an inlet-weighted sum. The time period and averaging are the same as in Figure 21. (Notice that the black curve represents the combination element here but, in Figure 21, black represents the small rosette.)

CONCLUSIONS

The preliminary results of this work can be summarized as follows:

- Reasonable estimates for the magnitude and phase response of all four infrasound elements at I99 were made from 0.008 Hz to several hertz. The scatter in the results is higher than typical for similar measurements at more sheltered sites.
- For all four elements, from 0.01 to 0.1 Hz, the measured magnitude and phase correspond closely to the manufacturer's specifications for the MB2005. Above 1 Hz, the effects of the pipe system produce a significant change in the phase response compared to the MB2005. Below 0.01 Hz, the phase also changes somewhat faster than expected (as if there is another pole at very low frequency in the system).
- Resonance suppressors are installed in all four elements; however, both the magnitude and phase response of the small rosette element show indications of an incompletely suppressed resonance above a few hertz.
- A preliminary investigation of the effects of non-acoustic turbulence and the associated scale sizes was performed and an apparent drop in the magnitude response of the larger elements below 0.08 Hz was tentatively associated with area-averaging of non-acoustic pressure fluctuations.
- Non-acoustic fluctuations may be useful for determining element response at very low frequency – below 0.05 Hz – even in windy conditions.
- The effects of inlet distribution particularly for the large hexagonal element appear to be more complicated than simple incoherent summation of isotropic turbulence: in windy conditions, the large hexagonal element showed higher spectral levels from 0.2 to 3 Hz than the small element but a virtual element formed by coherent summation of the large and small hexagons showed levels more consistent with expectations.
- Aside from the caveat above, the wind-noise-reduction performance of the various elements seems consistent with a model based on overall dimension for the lower frequencies and on inlet density for the middle frequencies.

ACKNOWLEDGEMENTS

These measurements would not have been possible without the support of Patrick Grenard, Ekrem Demirovic, Pavel Martysevich, Viatcheslav Bereza, Reinhard Jelinek, and Eva Graham of the CTBTO/PTS and Norbert Blaumoser of the ZAMG (Conrad Observatory). The CTBTO provided the travel and living expenses and the US Army Space and Missile Defense Command provided the salary support.

REFERENCES

Bowman, J. R., G. E. Baker, and M. Bahavar (2005). Ambient infrasound noise, *Geophys. Res. Lett*. 32: L09803.